

SACA: A Scenario-Aware Collision Avoidance Framework for Autonomous Vehicles Integrating LLMs-Driven Reasoning

Shiyue Zhao, Junzhi Zhang, Neda Masoud, Heye Huang, Xingpeng Xia, and Chengkun He

Abstract—Reliable collision avoidance under extreme situations remains a critical challenge for autonomous vehicles. While large language models (LLMs) offer promising reasoning capabilities, their application in safety-critical evasive maneuvers is limited by latency and robustness issues. Even so, LLMs stand out for their ability to weigh emotional, legal, and ethical factors, enabling socially responsible and context-aware collision avoidance. This paper proposes a scenario-aware collision avoidance (SACA) framework for extreme situations by integrating predictive scenario evaluation, data-driven reasoning, and scenario-preview-based deployment to improve collision avoidance decision-making. SACA consists of three key components. First, a predictive scenario analysis module utilizes obstacle reachability analysis and motion intention prediction to construct a comprehensive situational prompt. Second, an online reasoning module refines decision-making by leveraging prior collision avoidance knowledge and fine-tuning with scenario data. Third, an offline evaluation module assesses performance and stores scenarios in a memory bank. Additionally, A precomputed policy method improves deployability by previewing scenarios and retrieving or reasoning policies based on similarity and confidence levels. Real-vehicle tests show that, compared with baseline methods, SACA effectively reduces collision losses in extreme high-risk scenarios and lowers false triggering under complex conditions. Project page: <https://sean-shiyuez.github.io/SACA/>.

I. INTRODUCTION

Imagine an **extreme scenario**: a self-driving car speeding toward an intersection as the light turns green. Suddenly, a truck barrels through a fading yellow from the left, while pedestrians inch across the crosswalk ahead (see Fig. 1). What's the right move? Traditional collision avoidance systems, whether rule-based [1] or powered by reinforcement learning (RL) [2], often falter here, constrained by rigid mathematical frameworks.

These systems hinge on clear-cut objectives: rule-based approaches lean on preset thresholds to trigger actions [3], while RL methods encode priorities in reward functions [2]. While effective in predictable environments, these systems often fail in chaotic, high-stakes scenarios where adaptability is critical. Mathematical models alone often prove inadequate for navigating the complex interplay of physical dynamics, legal boundaries, and ethical dilemmas. Even end-to-end autonomous driving systems, built on deep neural networks that map camera feeds straight to steering, stumble in these

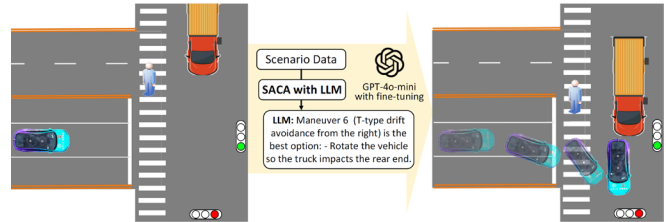


Figure 1. High-risk intersection scenario with an autonomous vehicle (in blue) facing a truck (in red) and pedestrians. SACA.

unseen scenarios [4]. They shine in everyday traffic but fail to generalize to rare, complex driving situations where training data is scarce [5]. Plus, their black-box nature makes it nearly impossible to weave in broader concerns, like societal norms or legal accountability, when lives hang in the balance [6]. So, here's the question: **How can we develop a reliable collision avoidance system for extreme collision avoidance scenarios that integrates safety and ethical considerations?** Rule-based logic lacks the flexibility to handle unforeseen events, and RL requires extensive trial-and-error to learn rare events. There is a need for a smarter approach—one that merges expert-level collision avoidance intuition with a broader contextual understanding of the real world.

To overcome these shortcomings, we develop a large language model (LLMs) methods. Our idea is to tap into LLMs for scenario-aware reasoning, pairing them with a preview-based strategy to boost real-world deployability. Recent models like ChatGPT-4 and Grok have shown off their ability for grasping **general world knowledge, human emotions, and near-human reasoning skills**. For instance, GPT-4 has demonstrated human-like judgment in ethical dilemmas, as seen in moral scenario evaluations, and even outpaced humans in empathy, according to a 2024 study [7]. Furthermore, LLMs stand out because they can spell out their reasoning step-by-step, offering a window into their decisions that end-to-end neural networks can't match.

Still, two key challenges stand out:

- **How can we incorporate collision avoidance expertise and experience such as analyzing obstacles and predicting motion, into LLMs' reasoning?**
- **How do we adjust these models to handle safety-critical extreme scenarios where fast decisions are essential and mistakes can't happen?**

S. Zhao, J. Zhang, and C. He are with School of Vehicle and Mobility, Tsinghua University, Beijing 100084 China (+1-734-210-9574; e-mail: thu_znqzd@163.com).

S. Zhao is now invited as a visiting scholar in the Department of Civil and Environmental Engineering, University of Michigan, Ann Arbor, MI 48105 USA.

N. Masoud and X. Xia are with the Department of Civil and Environmental Engineering, University of Michigan, Ann Arbor, MI 48105 USA.

H. Huang is with the Connected & Autonomous Transportation Systems Lab, University of Wisconsin-Madison.

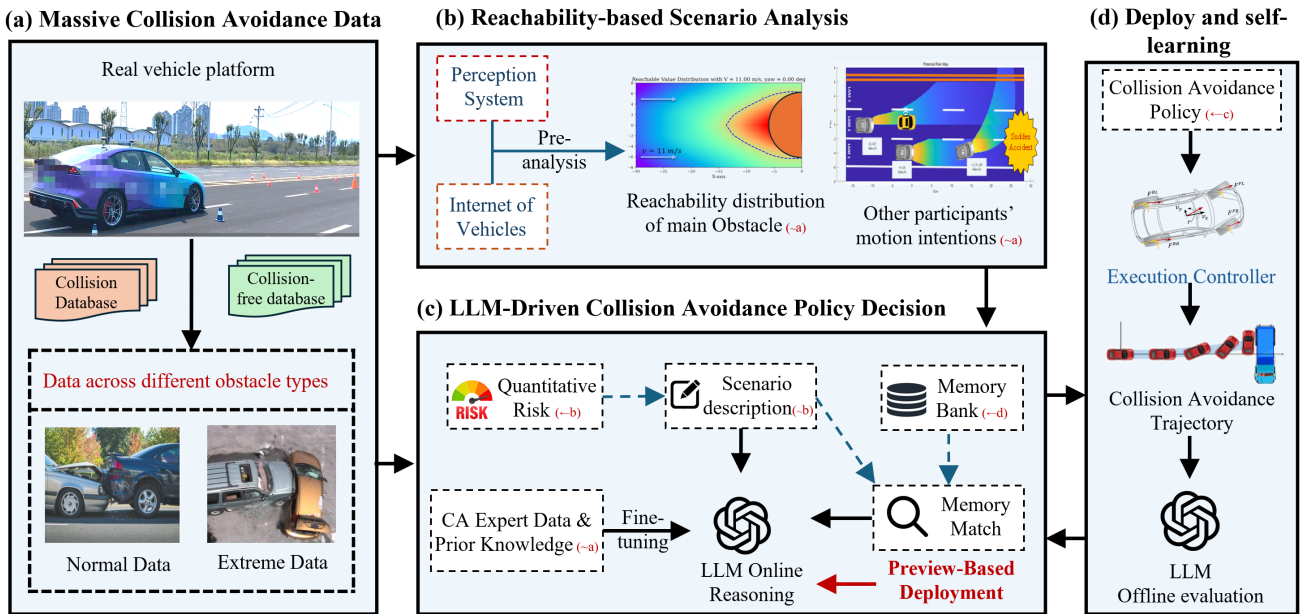


Figure 2. Overview of the LLM-driven Scene-Aware Collision Avoidance (SACA) framework. Arrows indicate direct outputs from a module, while the tilde (~) denotes related computations.

To address these, we introduce the Scenario-Aware Collision Avoidance (SACA) framework for **extreme collision avoidance scenarios**. Built on scenario awareness, LLMs, and scenario previews, SACA seeks to enhance decisions and ensure real-world reliability. This work makes three key contributions:

- (1) **Robust LLM Adaptation via Fine-Tuning:** By fine-tuning with memory-based retrieval, our framework reliably handles safety-critical extreme scenarios and enables continuous improvements.
- (2) **Scenario-Aware Risk Assessment for Collision Avoidance:** Through obstacle reachability analysis and traffic participant intention prediction, we construct a contextual model to guide LLMs.
- (3) **Scenario-Preview-Based Deployment:** SACA leverages a memory bank of scenarios and precomputed policies for low-latency deployment, adapting to extreme situations.

As an illustrative example, Fig. 1 presents a high-risk intersection scenario where an autonomous vehicle (blue) encounters a truck (red) running a yellow light and nearby pedestrians. Leveraging SACA’s fine-tuned *GPT-4o-mini*, the vehicle performs a T-type drift maneuver, shifting right to minimize collision impact and ensure pedestrian safety.

II. RELATED WORK

Risk Assessment and Motion Intention Recognition:

Research on obstacle and traffic participant risk assessment in autonomous driving relies on key theoretical frameworks, each with distinct challenges. The artificial potential field (APF) method, pioneered by Khatib [8], models risks using potential fields to represent obstacles as repulsive forces and goals as attractive ones, with Huang et al. [9] extending this to integrate road, vehicle, and velocity dynamics for collision avoidance. Still, these approaches tend to overlook aspects like the ego vehicle’s execution capability and its operational status. Another approach, Hamilton–Jacobi (HJ) reachability analysis,

offers a rigorous framework by identifying backward reachable sets—states where collisions with obstacles or traffic participants become unavoidable—while accounting for ego vehicle dynamics [10]. Li et al. [11] enhance HJ reachability by clustering vehicle behaviors (e.g., left/right turns) via trajectory prediction, yielding less conservative HJ-based controllers tested in T-intersections and roundabouts. Still, its heavy computational demands in high-dimensional settings, known as the “curse of dimensionality,” make real-time application difficult [18]. For traffic participants, particularly nearby vehicles, motion intention recognition has progressed through model-based techniques like Hidden Markov Models (HMM) and data-driven methods, such as neural networks (e.g., LSTM, deep belief networks) [13], trained on datasets like NGSIM to better predict lane changes or lane-keeping actions.

LLMs-based Decision-making for autonomous Driving:

Recent work has highlighted how LLMs are making strides in autonomous driving decisions. Jiao Chen et al. [14] proposed with EC-Drive, an edge-cloud setup that taps LLMs like GPT-4 to handle key driving data, cutting down on delays and boosting efficiency in real-world conditions. A VLM-MPC framework proposed by Long et al. [15] blends Vision Language Models with real-time control, using nuScenes data to keep vehicles safe in complex settings like rain or busy intersections. Zheng et al.’s PlanAgent [16] used a Multi-modal LLM to tackle rare, complex cases, outperforming top methods on nuPlan tests through step-by-step reasoning. Sha et al. [17] showed in LanguageMPC that LLMs can act as smart decision-makers, outperforming standard approaches in managing single and multiple vehicles with their practical know-how. Wang et al. [18] explored LLMs for planning, adding a safety check to improve outcomes in unpredictable simulations. Huang et al. [19] presented SafeDrive, a risk-sensitive decision-making framework that integrates knowledge- and data-driven approaches to enhance human-like decision-making in high-risk and long-tail scenarios.

However, incorporating driving expertise and ensuring that LLMs operate smoothly in the real world remains a major hurdle, as some studies have pointed out that LLMs require extensive traffic perception knowledge and are slow to react at critical moments [20]. Our SACA framework addresses these gaps, using LLMs to achieve intelligent and practical collision avoidance in extreme driving situations.

III. FRAMEWORK

This study proposes SACA, an LLM-driven collision avoidance policy arbitration and decision-making framework (Fig. 2), built on real-vehicle scenarios and a pre-developed policy library [1, 21–23]. Aiming to minimize collision loss, SACA integrates legal, ethical, and emotional factors to select optimal strategies through scenario analysis, LLM reasoning, and real-time deployment. The chosen policy is executed by the control module, with outcomes evaluated offline and stored for continual self-learning. Table I lists candidate collision avoidance policies. Policies 3 and 4 involve coordinated braking and steering without inducing high-slip conditions, enabling lateral movement with quick directional recovery. SACA outputs target velocities for these policies. Policies 5 and 6 involve T-type drift maneuvers, deliberately inducing lateral sliding to rapidly reorient and decelerate the vehicle. These are beneficial in lateral collision scenarios (T-type collision), redirecting impacts to energy-absorbing zones to protect occupants and the battery pack.

Within the LLM-driven decision-making module (Fig. 2c), the scenario descriptions obtained from reachability-based analysis (Fig. 2b) form the input prompts. Vector-based scene matching then compares the current scenario to stored cases in the memory bank, retrieving historically successful collision avoidance results as incremental reasoning prompts. Additionally, expert-annotated avoidance examples and key safety constraints are integrated via fine-tuning, enhancing the LLM’s adaptability to diverse collision scenarios. After execution, the outcome is evaluated offline and fed back into the memory bank, enabling iterative self-learning.

To address real-time constraints during deployment, a precomputed strategy approach is designed, enabling the previewing of scenarios and retrieving or reasoning policies based on similarity and confidence levels, thereby improving the real-time performance of execution.

TABLE I. CANDIDATE COLLISION AVOIDANCE POLICIES

ID	Name	Description	Ref.
0	AEB	Engages maximum braking force to stop the vehicle.	-
1	AES-L	Executes a sudden left turn to change lanes and resume direction.	[21]
2	AES-R	Executes a sudden right turn to change lanes and resume direction.	[21]
3	ES-B-L	Changes lanes to the left while applying braking.	[1]
4	ES-B-R	Changes lanes to the right while applying braking.	[1]
5	T-D-L	Performs a T-type drift maneuver, bringing the vehicle to a perpendicular stop facing left.	[22]
6	T-D-R	Performs a T-type drift maneuver, bringing the vehicle to a perpendicular stop facing right.	[22]
7	NI	The situation does not require intervention.	-

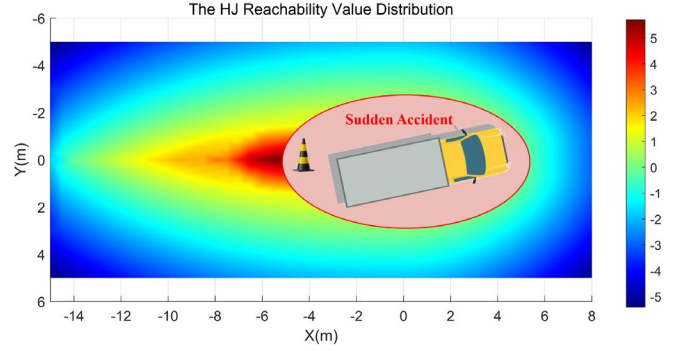


Figure 3. HJ reachability value distribution for an elliptical obstacle. The red ellipse indicates the obstacle boundary. The color gradient represents reachability values, defined as Formula 1. Positive values indicate intrusion into the obstacle envelope, with higher values signifying greater risk.

IV. METHODOLOGY

This section looks at how the SACA framework integrates specialized collision avoidance knowledge to support real-time, flexible decision-making. Essentially, it explains how to address the two major challenges of reliability and real-time deployment raised in Section I.

A. Predictive Scenario Analysis

LLM requires input to describe scenarios incorporating collision avoidance expertise, thus requiring prior risk assessment and motion prediction to make informed decisions.

Obstacle Reachability Analysis: For obstacles with relatively fixed motion states, such as sudden accident vehicles, SACA uses Hamilton–Jacobi (HJ) reachability to gauge the danger they pose to the ego vehicle’s operation. The reachable value, reflected in functions like $V_h(x)$ and $Q_h(x, u)$ indicates how well the vehicle can avoid such obstacles starting from the current state x , focusing solely on evasion.

$$V_h(x) = \min_{u(\cdot)} [\max_{\tau \in N} h(x_\tau)], x(0) = x \quad (1)$$

$$Q_h(x, u) = \min_{u(\cdot)} [\max_{\tau \in N} h(x_\tau)], x_0 = x, u_0 = u \quad (2)$$

where state x includes vehicle dynamics, and control u refers to steering and throttle/braking. The state x_τ at time τ is evaluated as unsafe $h(x_\tau) \geq 0$ (e.g., collisions), or safe $h(x_\tau) < 0$. Due to computational challenges of high-dimensional HJ reachability, SACA leverages a database (31+ million real-world samples) and offline RL [23] to approximate $V_h(x)$ and $Q_h(x, u)$ via neural networks, using the reachability Bellman operator:

$$\mathcal{B}^* Q_h(x, u) := (1 - \gamma)h(x) + \gamma \max\{h(x), V_h^*(x')\} \quad (3)$$

The approximate Bellman operator satisfies the contraction property, allowing value iteration. Using collected data, offline reinforcement learning yields a neural network that approximates reachable values $V_h(x)$. Once deployed, this network computes real-time risk levels for relevant obstacles, integrating ego vehicle capability-aware risk into the SACA framework. Fig. 3 illustrates the risk distribution for an elliptical obstacle. Reachable values are normalized to quantify risk across obstacles using:

$$R(x) = \frac{V_h(x) - V_h^{min}}{V_h^{max} - V_h^{min}} \quad (\text{mapped to } [0,1]) \quad (4)$$

where V_h^{max} and V_h^{min} are manually set sensitivity adjustment parameters. This process incorporates risk data accounting for the ego vehicle’s operational capabilities into the SACA.

Traffic Participants Motion Intention Prediction [2]:

Reachability analysis effectively gauges risks from obstacles with relatively stable motion states by leveraging the ego vehicle’s dynamics and operational capabilities. However, for participants like surrounding vehicles, whose motion states can change rapidly, their intentions become a crucial factor. For instance, two vehicles with the same position and speed present very different risks if one maintains course while the other performs an emergency brake. This contrast underscores why we must integrate motor intention into LLM inputs, with surrounding vehicles as a prime example.

Many collisions stem from sudden longitudinal or lateral maneuvers, such as lane changes or braking. To address this, we propose an intention recognition method that classifies surrounding vehicles’ motions (I) into six categories: Maintain (M), forward braking (FB), left braking (LB), left lane change (LC), right braking (RB), and right lane change (RC). Formally:

$$I \in I_{all} = [M, LC, RC, FB, LB, RB] \quad (5)$$

We predict these intentions using a hybrid Long Short-Term Memory (LSTM) and Conditional Random Field (CRF) model, drawing on recent time-series driving data (e.g., speed, steering, pedal inputs). The LSTM processes these inputs to estimate intentions:

$$\tilde{I}_t = LSTM(D_t, D_{t-1}, \dots) \quad (5)$$

where D_t represents the driving input data at time t . However, the LSTM alone overlooks logical transitions in consecutive intentions—e.g., a vehicle is unlikely to shift abruptly from LB to RB. CRF enforces consistency through a transition matrix A where $a_{ij} = P(I_t = I_{all}(j) | I_{t-1} = I_{all}(i))$, derived from expert knowledge [4]. As a result, the final output I_t retains LSTM’s sensitivity to continuous driving patterns while incorporating real-world constraints on adjacent intention transitions.

This LSTM-CRF approach supports detection of sudden braking or lane changes, enhancing collision risk assessment when used alongside reachability analysis. Though this study focuses on vehicles, it can be extended to other road users with appropriate motion models.

Prompt Organization for Scenario Description: SACA employs a structured scene description prompt to guide the LLM, integrating the ego vehicle’s state (e.g., position $([0, 0])$, velocity 28 m/s), reachability-based obstacle risk (e.g., small car, risk 0.33), and traffic participant intentions (e.g., Maintain or Forward Braking) identified by LSTM-CRF. The results analysis in Section IV illustrates how these prompt elements are organized, detailing the ego vehicle’s context, obstacle parameters (e.g., a 5 m axis), and participant actions.

B. Fine-Tuning and Case-Based Reasoning

We introduce a dual strategy that combines supervised fine-tuning (SFT) with case-based reasoning (CBR) into SACA. Through fine-tuning, the LLMs in SACA internalize domain-specific collision avoidance knowledge, physics-based rules, and common scenario data, enabling it to function like a seasoned “collision avoidance expert.” Complementing this, the CBR serves as a “living notebook,” allowing retrieval of past successes and failures to guide decisions in rare or extreme conditions.

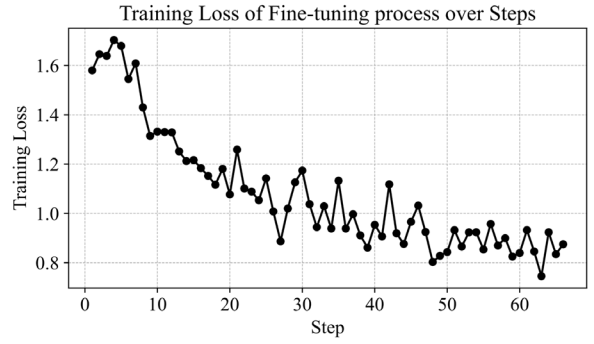


Figure 4. Training loss curve for fine-tuning GPT-4o-mini-2024-07-18, illustrating consistent convergence over the training steps.

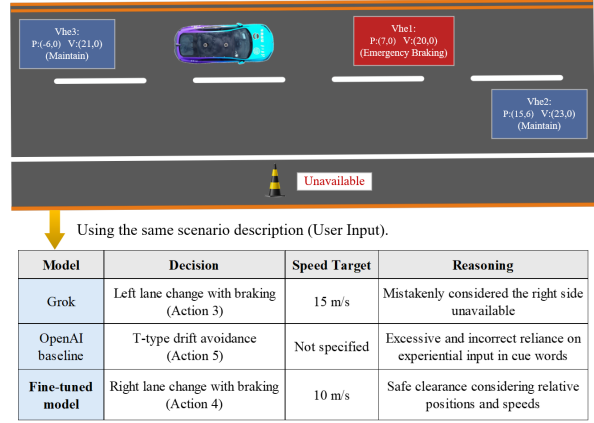


Figure 5. Decision outcomes of Grok, OpenAI baseline, and the fine-tuned LLM in a frontal emergency-braking scenario.

We performed supervised fine-tuning on the GPT-4o-mini-2024-07-18 model using OpenAI’s recommended pipeline and hyperparameter settings. The training corpus consisted of domain-specific question–answer pairs derived from over 50 collision cases selected with reference to the NHTSA Fatality Analysis Reporting System (FARS), covering various highway, intersection, and ramp scenarios, along with expert reasoning demonstrations ([The dataset will be made public in the project files after publishing](#)). In total, we used 235,284 training tokens, which met the fine-tuning guidelines of OpenAI. Fig. 4 shows a consistently declining loss curve, indicating effective convergence.

Compared to baseline GPT-4o-mini and Grok models, our fine-tuned LLMs exhibits notably enhanced spatial perception and domain-specific collision avoidance reasoning, such as estimating breaking distances. As illustrated in Fig. 5, given identical scenario inputs and expert guidance, Grok produces sub-optimal decisions due to its limited scenario understanding (policy 3), and GPT-4o-mini baseline mistakenly suggests a T-type drift (policy 5). These choices indicate a misunderstanding of spatial constraints and an improper application of expert guidance. Our model with fine-tuning correctly evaluates the spatial limitations and the risk presented by the trailing vehicle, choosing policy 4 (a right lane-change with braking) to preserve a safe distance.

To enhance the proposed method, we incorporated a case-based reasoning mechanism, as depicted in Fig. 2. Each time SACA is activated, an independent LLM retrospectively

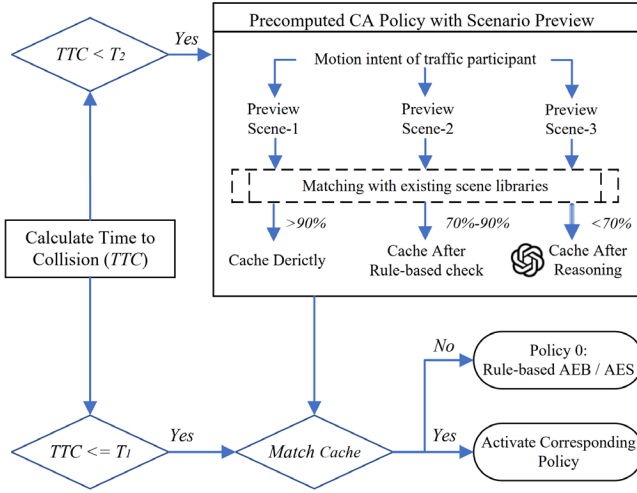


Figure 6. Scenario-preview-based deployment mechanism in SACA.

Algorithm 1: Scenario-Aware Collision Avoidance Integrating LLMs-Driven Reasoning

Input: Road geometry data, obstacle info (position & dimensions), surrounding vehicles' states (position, velocity, controls), thresholds T_1, T_2 , memory bank, fine-tuned LLM
Output: Selected collision avoidance policy ID, updated memory bank after action and evaluation
Compute current Time to Collision (TTC);
if $TTC < T_2$ **then**
 Conduct obstacle reachability analysis (e.g., Hamilton–Jacobi);
 Predict motion intentions of surrounding vehicles (e.g., lane change, braking);
 Forecast three potential collision scenarios at future time T_1 ;
 Generate structured scenario descriptions for each forecasted scenario;
 foreach forecasted scenario **do**
 Compare with existing scenarios in memory bank to get a similarity score;
 if similarity > 90% **then**
 Cache the corresponding policy immediately
 else if 70% < similarity ≤ 90% **then**
 Perform safety validation check, then cache the policy
 else
 Use fine-tuned LLM reasoning with the nearest scenario from memory bank;
 Cache the policy inferred by the LLM
 end
 end
 if current $TTC \leq T_1$ (collision avoidance trigger) **then**
 Match the current scenario with cached scenarios;
 if match similarity > 90% **then**
 Execute the cached collision avoidance policy
 else
 Execute the default rule-based emergency brake (Policy 0: AEB/AES)
 end
 end
end
After execution: perform offline evaluation of the trajectory and any collision outcomes using a dedicated LLM;
Update the memory bank with new scenario data and evaluation results for continuous improvement;

assesses the collision avoidance performance and evaluates collision losses. This process enables continuous improvement through online case-based self-learning.

C. Scenario-Preview-Based Deployment

We developed a scenario-preview-based deployment method (Fig. 6). This method initiates when the calculated time-to-collision (TTC) drops below a predefined threshold ($TTC < T_2$), prompting scenario previewing based on the current obstacle dynamics and predicted motion intentions of surrounding traffic participants.

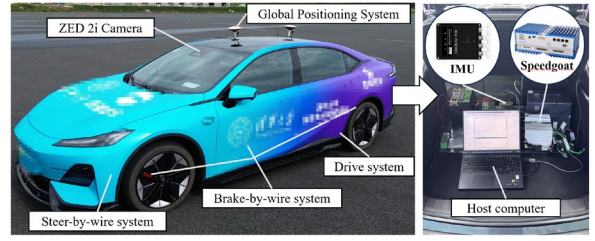


Figure 7. Test vehicle platform and its key components.

Preview Scenario at T_t
<p>AUTONOMOUS DRIVING COLLISION AVOIDANCE SCENARIO</p> <p>## Ego Vehicle: ID=ego, type=small car, position=(0.0, 0.0), velocity=(14.0, 0.0), Road Topology=Intersection</p> <p>## Obstacles: No static obstacles detected.</p> <p>## Traffic Participants: Participant ID=object1, type=Large Truck. The participant is 16.0 m in front of the vehicle and 6.4 m to the left. The participant is moving to the right at a speed of 7.5 m/s. Intention = FD (Maintain).</p> <p>Participant ID=pedestrian, type=pedestrian The participant is 6 m in front of the vehicle and 4 m to the left. The participant is moving to the left at a speed of 0 m/s. Intention = Maintain.</p> <p>## HISTORICAL SCENARIOS: No historical data is available.</p>
SACA Reasoning Process
<p>Scenario Analysis</p> <p>1. Ego Vehicle State: - The ego vehicle is traveling at 14 m/s in an intersection.</p> <p>2. Collision Target (Large Truck): - Located 16.0 m ahead and 6.4 m to the left. - Moving right at 8.0 m/s, crossing the ego vehicle's path. - TTC Calculation: $TTC = 16/14 = 1.23s$ - Since $TTC = 1.3s$, intervention is required.</p> <p>4. Collision Risk Assessment: - The truck's lateral movement means it will cross the ego vehicle's path imminently. - The pedestrian's position limits the use of leftward avoidance maneuvers.</p> <p>5. Decision Analysis: - Braking alone (Action 0) may not prevent a collision, - Leftward maneuvers (Actions 1, 3, 5) are not viable due to the pedestrian. - Rightward maneuvers (Actions 2, 4) are not viable, as they may not provide enough time to avoid - The impact should be directed to the energy-absorbing structure to protect the battery and occupants. - T-type drift avoidance to the right side (Action 6) is the safest option.</p> <p>Response to user: 6</p>

Figure 8. Validation of the SACA reasoning process at intersection.

It anticipates three potential collision scenarios at a future time ($TTC = T_1$), comparing them against previously stored scenarios. If similarity exceeds 90%, the existing collision avoidance policy is directly cached. If between 70% and 90%, a rule-based safety check is performed before caching. For similarities below 70%, LLM-based online reasoning generates and caches a suitable policy. At the decision-making time ($TTC < T_1$), the current scenario is compared with cached scenarios. A matching cached policy is immediately activated; otherwise, the system defaults to a rule-based

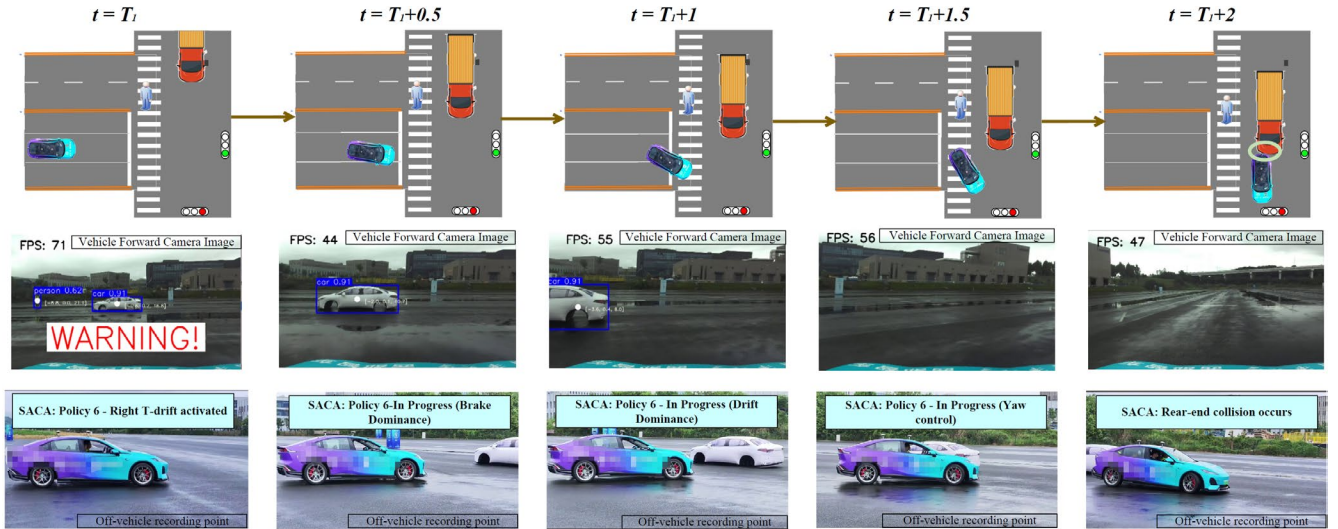


Figure 9. Real-vehicle experimental validation of the T-type drift collision avoidance maneuver in the intersection scenario.

emergency braking.

This preview mechanism significantly enhances real-time applicability by providing additional inference time ($T_2 - T_1$) for LLM reasoning, as verified using OpenAI’s API under optimal response conditions. Although current computational resources still constrain fully reliable LLM deployment, this framework offers a practical solution for incorporating LLM-driven decisions into critical collision avoidance tasks, improving upon prior approaches [19, 20].

In summary, SACA integrates scenario prediction, logical reasoning, and memory retrieval, as detailed in the provided pseudocode.

V. EXPERIMENTAL EVALUATION

To validate the effectiveness and deployability of the proposed SACA framework, real-world tests were conducted in critical collision scenarios.

A. Experimental Setup

The verification platform is a consumer-grade rear-wheel drive electric vehicle (Fig. 7) with a steer-by-wire system, torque-controlled drive system, and brake-by-wire system. It uses cameras, inertial navigation (CGI 610), and GNSS to track position, velocities, accelerations, yaw rate, and wheel speed in real time. Data is processed via CAN FD by a *Speedgoat* computer (Intel i7 2.5 GHz dual-core CPU, 8 GB RAM, high-speed I/O613 modules) for control commands. The main innovation of this work is SACA’s scenario-based arbitration for extreme collision avoidance. We compared its performance to two baselines:

- **LLMs without Fine-tuning:** Uses the same system architecture but skips domain-specific fine-tuning, relying on the LLM’s general reasoning.
- **Imitation Learning:** Based on [24], it trains a policy on expert data for high-risk collisions, without scenario reasoning or preview.

For safety and ego vehicle’s perception capabilities, the collision avoidance trigger ($TTC - T_1$) was set to 1.3 seconds.

Accounting for the LLM’s latency, the scenario preview and inference trigger ($TTC - T_2$) was set at 5.5 seconds.

B. Intersection Scenarios

In the intersection scenario, a mixed virtual-real approach ensured safety: a stationary vehicle simulated a high-speed lateral threat. Detected by the ego vehicle’s perception system, it was treated as moving dynamically. At $T_2 = 5.5$ s (scenario preview), the ego vehicle, traveling at 14 m/s, detected an inflatable car 55 m ahead via a ZED 2i camera. The virtual environment showed a truck 55 m ahead and 43 m left, moving laterally at 7.5 m/s, and a pedestrian 48 m forward and 8.2 m left, crossing at 1 m/s.

Fig. 8 illustrates SACA’s scenario preview and LLMs-driven reasoning. The upper part maps the environment at T_1 , detailing positions, speeds, and intentions of objects. The lower part shows the fine-tuned LLM processing this data, predicting the truck crossing the ego vehicle’s path in 1.3 s. With the pedestrian blocking leftward moves and braking insufficient, SACA opts for a rightward T-type drift (Action 6) to redirect collision forces into energy-absorbing structures, enhancing safety. Fig. 9 shows the T-type drift collision avoidance results in the intersection scenario. The schematic (top) tracks the truck, pedestrian, and ego vehicle positions from $t = T_1$ to $t = T_1 + 2$. Camera images (middle) confirm detection and warnings, while off-vehicle recordings (bottom) validate the drift, redirecting collision forces to the rear energy-absorbing structures, avoiding severe injuries.

We compared our method to two baselines from Section IV.A using identical preview settings. The ego vehicle’s speed varied from 10–15 m/s, and the truck simulated forward driving intention (intervention needed) or emergency braking intention (no intervention needed). Each scenario ran 10 times. Two metrics were tracked:

- **Collision Loss:** Calculated by multiplying collision-relative velocity with injury rates [25]: 0.41 (side), 0.35 (front), and 0.21 (rear).
- **False-Trigger Loss:** In no-risk cases, moderate maneuvers (Policy 0–4) cost 0.5, extreme drifts (Policy 5–6) cost 1.0, averaged over trials.

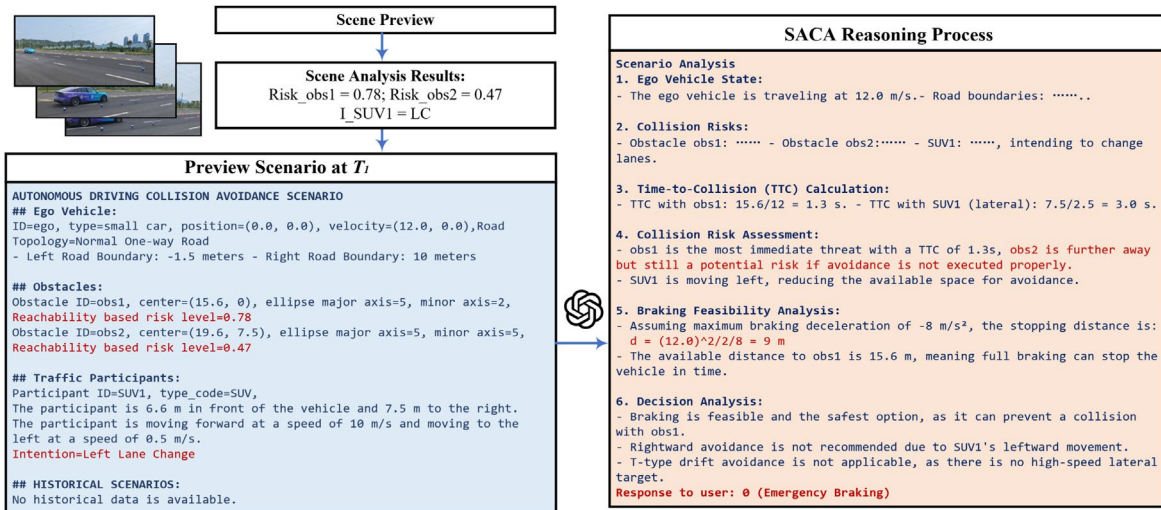


Figure 10. Scene preview and LLM-driven reasoning workflow under a one-way road scenario.

TABLE II. COMPARISON OF COLLISION LOSS AND FALSE-TRIGGER LOSS ACROSS TESTED METHODS IN INTERSECTION SCENARIOS.

Methods	Collision Loss	False-Trigger Loss
Imitation Learning [38]	2.36	0.35
LLMs without Fine-tuning	1.85	0.27
Our SACA	0.54	0.05

Comparison results (Table II) indicate that our SACA method achieves the lowest collision loss (1.54) while nearly eliminating false-trigger events. In contrast, imitation learning shows the highest collision loss (2.36) and moderate false-trigger rates. The LLM without fine-tuning exhibits intermediate collision loss (1.85) with a small yet non-zero false-trigger loss (0.27). These results demonstrate that fine-tuning and scenario-aware decision-making significantly enhance the reliability and accuracy of collision avoidance in extreme conditions.

C. One-way Road Scenarios

In this scenario, when reaching a time-to-collision threshold ($T_2 = 5.5$ s), the ego vehicle travels at 12 m/s along a multi-lane, one-way road. Ahead, an elliptical obstacle (major radius 3.5 m, minor radius 1.75 m) is located 66 m forward in the same lane, and a circular obstacle (radius 5 m) lies 70 m ahead and 7.5 m to the right. The road's left boundary is 1.5 m from the ego lane, and its right boundary is 10 m away, forming two additional lanes. Another vehicle, positioned 7.5 m to the right and 15 m ahead, is traveling at 10 m/s and intends to merge left.

In real-vehicle tests, red barriers represented obstacles, and blue barriers indicated lane boundaries and lane-change trajectories. To investigate the impact of scenario perception on decision-making, we introduced an additional baseline called **LLMs without Scenario-Awareness**, using identical LLM architecture but omitting the HJ-based risk analysis and motion intention recognition. Subsequent sections compare baseline methods against our SACA framework in obstacle and lane-change response.

Fig. 10 illustrates the scenario preview, risk assessment, and LLM reasoning process. Analysis indicates obstacle obs1

TABLE III. COMPARISON OF COLLISION LOSS AND FALSE-TRIGGER LOSS ACROSS TESTED METHODS IN ONE-WAY ROAD SCENARIOS.

Methods	Collision Loss	False-Trigger Loss
Imitation Learning	0.49	0.50
LLMs without Fine-tuning	1.06	0.20
LLMs without Scenario-Awareness	0.65	0
Our SACA	0.07	0

($TTC \approx 1.3$ s) presents the highest immediate collision risk, while obstacle obs2 poses a moderate threat. The surrounding SUV (I_SUV1) merging left further constrains available space. Given reachability-based risks (0.78 for obs1, 0.47 for obs2) and braking feasibility checks, SACA selects maximum braking (Policy 0) to safely stop before obs1, avoiding collision.

We conducted comparative tests using baseline methods described in Section IV.A, under identical preview conditions on the multi-lane, one-way road. The ego vehicle's initial speed was fixed at 12 m/s, and obstacles and surrounding vehicles were positioned consistently. Each method underwent 10 repeated trials under collision-risk and no-collision-risk conditions. The no-collision-risk (false-trigger) scenarios replicated collision-risk setups but removed the primary forward obstacle to evaluate false-trigger occurrences. Results are summarized in Table III.

Quantitative analysis indicates that SACA achieves the lowest average collision loss (0.0697), significantly outperforming all baseline methods. The imitation learning method consistently triggers identical maneuvers (Policy 4), resulting in repeated minor collisions at low speeds (1.2 m/s) and thus a higher collision loss (0.492). The LLM without fine-tuning exhibits inconsistent maneuver choices, resulting in the highest collision loss (1.06). Meanwhile, the LLM without scenario-awareness yields moderate collision loss (0.656), frequently selecting maneuvers without integrated braking. Additionally, lacking scenario-awareness, this method cannot accurately perceive that the SUV on the right is merging left, potentially blocking the right-side escape route. Consequently,

TABLE IV. COMPARISON OF COLLISION LOSS AND FALSE-TRIGGER LOSS ACROSS TESTED METHODS IN ONE-WAY ROAD SCENARIOS.

Scenario	Avg. Response Token	Avg. Response Time (s)	Min. Response Time (s)
Intersection Scenarios	371	5.7	3.7
One-Way Road Scenario	352	5.3	3.5

it opts for a rightward lane-change maneuver, increasing collision risk and thus collision loss.

In false-trigger tests, SACA and LLM without scenario-awareness correctly identify scenarios requiring no intervention, resulting in zero false-trigger loss. However, imitation learning consistently misinterprets these scenarios, unnecessarily performing lane-change maneuvers (Policy 4) and accruing moderate false-trigger loss (0.50). The LLM without fine-tuning occasionally misjudges situations, leading to unnecessary interventions (Policies 2 and 4) and a lower yet non-zero false-trigger loss (0.20).

D. Real-Time Feasibility

We evaluated real-time feasibility by analyzing inference durations for intersection and one-way road scenarios. Both scenarios set preview initiation time T_2 at 5.5 s and collision avoidance trigger T_1 at 1.3 s, providing a maximum inference window of 4.2 s.

Inference times and token lengths are summarized in Table IV. Only episodes completing inference within 4.2 s were considered for previous performance analyses. Although average inference times exceed 4.2 s, the minimum times confirm that SACA can reliably meet real-time constraints under optimal API response conditions.

VI. CONCLUSION

This study proposes the Scenario-Aware Collision Avoidance (SACA) framework, integrating Large Language Models (LLMs), predictive risk assessment, and memory-based decision-making for autonomous vehicles. SACA uniquely integrates ethical and legal factors with collision avoidance expertise, achieving a **70.8%–93.4%** reduction in collision loss and an **81.5%–100%** reduction in false-trigger loss compared to baselines in tested scenarios, while maintaining real-time performance under optimal API response conditions. The primary limitation remains the inference speed of LLMs. Future research should explore edge computing architectures or regional cloud computing centers to optimize model efficiency, enhance scenario databases, and integrate advanced perception systems, further improving performance and applicability. Overall, integrating LLMs into intelligent transportation systems holds great potential, promising safer and more ethically aligned autonomous driving solutions.

REFERENCES

[1] S. Zhao, J. Zhang, C. He, M. Huang, Y. Ji, and W. Liu, "Collision-free emergency planning and control methods for CAVs considering intentions of surrounding vehicles," *ISA Trans.*, vol. 136, pp. 535–547, 2023.

[2] Y.-H. Hsu and R.-H. Gau, "Reinforcement learning-based collision avoidance and optimal trajectory planning in UAV communication

networks," *IEEE Trans. Mobile Comput.*, vol. 21, no. 1, pp. 306–320, 2020.

[3] G. Li *et al.*, "Risk assessment-based collision avoidance decision-making for autonomous vehicles in multi-scenarios," *Transp. Res. Part C Emerg. Technol.*, vol. 122, p. 102820, 2021.

[4] F. Codevilla, M. Müller, A. López, V. Koltun, and A. Dosovitskiy, "End-to-end driving via conditional imitation learning," in *Proc. IEEE Int. Conf. Robot. Autom. (ICRA)*, 2018: IEEE, pp. 4693–4700.

[5] A. Bewley *et al.*, "Learning to drive from simulation without real world labels," in *Proc. IEEE Int. Conf. Robot. Autom. (ICRA)*, 2019: IEEE, pp. 4818–4824.

[6] L. Chen, P. Wu, K. Chitta, B. Jaeger, A. Geiger, and H. Li, "End-to-end autonomous driving: Challenges and frontiers," *IEEE Trans. Pattern Anal. Mach. Intell.*, vol. 46, no. 12, pp. 10164–10183, Dec. 2024.

[7] A. Welivita and P. Pu, "Are Large Language Models More Empathetic than Humans?," *arXiv preprint arXiv:2406.05063*, 2024.

[8] O. Khatib, "Real-time obstacle avoidance for manipulators and mobile robots," in *Proc. IEEE Int. Conf. Robot. Autom. (ICRA)*, vol. 2, 1985, pp. 500–505.

[9] H. Huang *et al.*, "General optimal trajectory planning: Enabling autonomous vehicles with the principle of least action," *Eng.*, vol. 33, pp. 63–76, 2024.

[10] S. Bansal, M. Chen, S. Herbert, and C. J. Tomlin, "Hamilton-Jacobi reachability: A brief overview and recent advances," in *Proc. IEEE Conf. Decis. Control (CDC)*, 2017, pp. 2242–2253.

[11] A. Li, L. Sun, W. Zhan, M. Tomizuka, and M. Chen, "Prediction-based reachability for collision avoidance in autonomous driving," in *Proc. IEEE Int. Conf. Robot. Autom. (ICRA)*, 2021, pp. 7908–7914.

[12] S. Bansal and C. J. Tomlin, "DeepReach: A deep learning approach to high-dimensional reachability," in *Proc. IEEE Int. Conf. Robot. Autom. (ICRA)*, 2021, pp. 1817–1824.

[13] A. Zyner, S. Worrall, J. Ward, and E. Nebot, "Long short term memory for driver intent prediction," in *Proc. IEEE Intell. Veh. Symp. (IV)*, 2017, pp. 1484–1489.

[14] J. Chen, S. Dai, F. Chen, Z. Lv, and J. Tang, "Edge-Cloud Collaborative Motion Planning for Autonomous Driving with Large Language Models," *arXiv preprint arXiv:2408.09972*, 2024.

[15] K. Long, H. Shi, J. Liu, and X. Li, "VLM-MPC: Vision Language Foundation Model (VLM)-Guided Model Predictive Controller (MPC) for Autonomous Driving," *arXiv preprint arXiv:2408.04821*, 2024.

[16] Y. Zheng *et al.*, "Planagent: A multi-modal large language agent for closed-loop vehicle motion planning," *arXiv preprint arXiv:2406.01587*, 2024.

[17] H. Sha *et al.*, "Langagempc: Large language models as decision makers for autonomous driving," *arXiv preprint arXiv:2310.03026*, 2023.

[18] Y. Wang *et al.*, "Empowering autonomous driving with large language models: A safety perspective," *arXiv preprint arXiv:2312.00812*.

[19] Z. Zhou, H. Huang, B. Li, S. Zhao, and Y. Mu, "SafeDrive: Knowledge- and Data-Driven Risk-Sensitive Decision-Making for Autonomous Vehicles with Large Language Models," *arXiv preprint arXiv:2412.13238*, 2024.

[20] C. Cui, Y. Ma, X. Cao, W. Ye, and Z. Wang, "Receive, reason, and react: Drive as you say, with large language models in autonomous vehicles," *IEEE Intell. Transp. Syst. Mag.*, vol. 16, no. 4, pp. 81–94, 2024.

[21] J. Han *et al.*, "Uniform finite time safe path tracking control for obstacle avoidance of autonomous vehicle via barrier function approach," *IEEE Trans. Intell. Transp. Syst.*, vol. 25, no. 8, pp. 9512–9523, Aug. 2024.

[22] X. Hou, J. Zhang, C. He, C. Li, Y. Ji, and J. Han, "Crash mitigation controller for unavoidable T-bone collisions using reinforcement learning," *ISA Trans.*, vol. 130, pp. 629–654, 2022.

[23] Y. Zheng *et al.*, "Safe offline reinforcement learning with feasibility-guided diffusion model," *arXiv preprint arXiv:2401.10700*, 2024.

[24] Z. Cao *et al.*, "Reinforcement learning based control of imitative policies for near-accident driving," *arXiv preprint arXiv:2007.00178*, 2020.

[25] National Highway Traffic Safety Administration, "Traffic safety facts 2022 data: Crash overview," U.S. Dept. Transp., Washington, DC, Rep. DOT HS 813 643, 2023. [Online]. Available: <https://crashstats.nhtsa.dot.gov/Api/Public/ViewPublication/813643>